

Surface-Derivatized Nanoceria with Human Carbonic Anhydrase II Inhibitors and Fluorophores: A Potential Drug Delivery Device

Swanand Patil,[†] Serge Reshetnikov,^{‡,||} Manas K. Haldar,[§] Sudipta Seal,^{*,†} and Sanku Mallik^{*,§}

Advanced Materials Processing and Analysis Center (AMPAC) and Nanoscience Technology Center, University of Central Florida, Orlando, Florida 32816, Duke University, Durham, North Carolina 27708, and Department of Pharmaceutical Sciences, North Dakota University, Fargo, North Dakota 58105

Received: November 17, 2006; In Final Form: April 16, 2007

Human carbonic anhydrase (hCAII) is a metalloenzyme that catalyzes the reversible hydration of carbon dioxide to bicarbonate and is associated with glaucoma (a major cause of blindness). The present study focuses on the use of cerium oxide nanoparticles (nanoceria) as a potential delivery device for hCAII inhibitors. Carboxybenzenesulfonamide, an inhibitor of the hCAII enzyme, was attached to nanoceria particles using epichlorohydrin as an intermediate linkage. Along with the CA inhibitor, a fluorophore (carboxyfluorescein) was also attached on the nanoparticles to enable the tracking of the nanoparticles in vitro as well as in vivo. X-ray photoelectron spectroscopic studies carried out at each reaction step confirmed the successful derivatization of the nanoceria particles. The attachment of carboxyfluorescein was also confirmed by confocal fluorescence microscopy. Preliminary studies suggest that carboxybenzenesulfonamide-functionalized nanoceria retains its inhibitory potency for hCAII.

Introduction

Countless individuals suffer from the ocular disease glaucoma. This condition describes a destruction of optic nerve cells and deterioration of eyesight as a result of increased intraocular pressure. The pressure is caused in part by a buildup of carbon dioxide in the eye. An enzyme that aids in the production of CO₂ is human carbonic anhydrase II (hCAII). This Zn²⁺-containing metalloenzyme (Figure 1) catalyzes the reversible hydration of carbon dioxide to bicarbonate and is commonly found in living organisms.

Sulfonamide compounds have been shown to selectively inhibit hCAII even at low concentrations.¹ Therefore, inhibition of hCAII with sulfonamides constitutes one of the most physiological approaches for treatment of glaucoma. In 1958, Beasley et al. reported the in vitro binding of 4-carboxybenzene sulfonamide (CBS) to the carbonic anhydrase (CA) enzymes.² Since then, many other hCAII inhibitors based on this moiety have been reported.^{3–5} A remarkable increase in the hCAII inhibition activity was observed for simple aliphatic ester of CBS.⁵ Also, it is now extensively documented that significant enhancement of CA inhibition can be achieved through coupling the primary recognition aromatic sulfonamide motif with secondary binding elements.^{3,5–9} The mechanism for inhibition of hCAII by CBS involves coordination of the sulfonamide group (as the anion) to the zinc atom in the active site of hCAII to form a complex in an exothermic reaction.^{6,10,11}

In treating ophthalmic diseases such as glaucoma, conventional liquid eye drops is not a sufficient mode of therapy because of lachrymal drainage losses. Because of the high

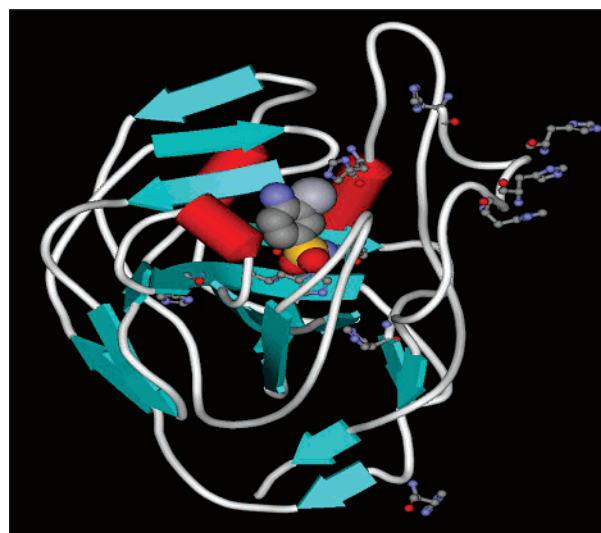


Figure 1. Cartoon diagram showing the structure of human carbonic anhydrase.

elimination rate, only a very small amount of about 1–3% of the dosage actually penetrates through the cornea and is able to reach intraocular tissues.^{12–14} Use of nanoparticles represents promising drug carriers for ophthalmic applications. The colloidal nanoparticles may be applied in liquid form just like eye drop solutions. After optimal drug binding to the nanoparticles, the ocular bioavailability of many drugs is significantly enhanced in comparison to normal aqueous eye drop solutions.¹² Also, smaller particles improve the patient comfort during administration as a scratching feeling might occur with larger particles. Nanoparticles and microspheres of various synthetic polymers such as poly-butylcyanoacrylate,^{15,16} polylactic acid,¹⁷ polymethylmethacrylate,¹⁶ and so forth as well as natural biocompatible polymers like albumin^{18,19} have been used for ophthalmic drug delivery applications.

* To whom correspondence should be addressed. E-mail: sseal@mail.ucf.edu (S.S.).

[†] University of Central Florida.

[‡] Duke University.

[§] North Dakota University.

^{||} NSF-REU Student, 2006.

The focus of this study was inhibition of hCAII, which is a primary target enzyme for the treatment of glaucoma.⁸ Nanoceria, a nontoxic nanoparticle, was functionalized with hCAII inhibitors and was tested as a potential ophthalmic drug delivery tool. We have found various applications of cerium oxide nanoparticles in biotechnology. It was found that treatment with nanomolar concentrations of cerium oxide nanoparticles increases cell longevity²⁰ and protects the cells from damages caused by X-ray radiation²¹ and reactive oxygen species.²² These studies have revealed that nanoceria particles are nontoxic and contain favorable biocompatibility.

Our studies related to use of nanoceria to protect the retina from oxidative stress caused by reactive oxygen species showed that the nanoparticles injected in the vitreous showed efficacy far away in the retina.²² Moreover, the nanoceria's uptake in human lung fibroblast cells was shown to be faster than the physical transport to the cell²³ suggesting that these particles have favorable diffusive properties. Therefore, the CeO₂ nanoparticles seem like a very good candidate for serving as transport agents for the inhibitors. Since carbonic anhydrase II is a cytosolic (found in cellular cytoplasm) enzyme, the inhibitor-functionalized nanoceria were synthesized to allow easy entry into living cells.

The first step was to choose a molecule that can attach to the nanoceria and that can inhibit carbonic anhydrase. CBS (Figure 2a) was the primary choice on the basis of the literature data, where it is shown that these benzenesulfonamides can serve as inhibitors of carbonic anhydrases and can possess favorable carboxyl groups for attachment.^{8,24} It was hypothesized that binding these molecules to the nanoceria would create an effective inhibitor of carbonic anhydrase that can be transferred into the cytosol. Additionally, we also decided to attach a carboxyfluorescein molecule (Figure 2b) to visualize the cell permeation property of the nanoparticles through a confocal fluorescence microscope.²⁵

The attachment of carboxybenzenesulfonamide and carboxyfluorescein molecules to nanoceria was confirmed using X-ray photoelectron spectroscopy (XPS). The formation of the fluorophore-functionalized nanoparticles was further established through confocal fluorescence microscopy. Finally, the derivatized nanoceria were tested as inhibitors of the recombinant hCAII enzyme. This was accomplished by observing the effect of nanoparticles on the rate of hCAII-catalyzed hydrolysis of the substrate 4-nitrophenyl acetate.²⁶

Experimental Section

Functionalization of Cerium Oxide Nanoparticles (Scheme 1). *Reaction of CeO₂ Nanoparticles with Epichlorohydrin and Ammonia.* The 250 mg of cerium oxide nanopowder (obtained from Sigma-Aldrich Inc.) was suspended in 10 mL of 0.1 M NaOH solution for 5 min. Then, 5 mL of epichlorohydrin was added, followed by the addition of 0.5 mL of 2 M NaOH. The suspension was stirred at room temperature for 6–8 h. The reaction mixture was then centrifuged, and the supernatant was decanted. The nanoparticles were washed by water followed by centrifugation. This was done until the pH of the water was approximately 7.0. The nanoceria powder was then dried under vacuum. Next, the nanopowder was again suspended in water, 25 mL of 30% ammonium hydroxide solution was added, and the reaction mixture was stirred for 14 h. The product was purified by centrifugation, was washed with water, and was dried under vacuum again.

Reaction with Carboxybenzenesulfonamide and Carboxyfluorescein. The nanoparticles from the previous step were

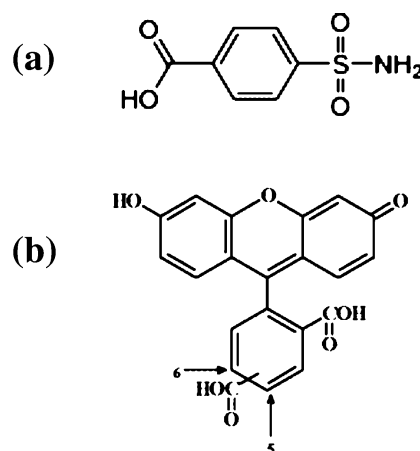


Figure 2. Molecular structure of (a) carboxybenzenesulfonamide and (b) carboxyfluorescein.

functionalized with the carboxybenzenesulfonamide and carboxyfluorescein molecules. These molecules (either 200 mg, 1 mmol of the CBS or carboxyfluorescein) were dissolved in 15 mL of dimethylformamide (DMF) and 5 mL of dichloromethane. Three hundred seventy-five microliters (3.5 mM) of *N*-methyl morpholine (NMP) was added followed by the addition of 442.5 mg (1 mmol) of the benzotriazol-1-yl-oxy-tris-(dimethylamino) phosphonium hexafluorophosphate (BOP) reagent. The reaction mixture was stirred for 10 min at room temperature. The nanoparticles were then added. The mixture was stirred for approximately 20 h at room temperature. The reaction was stopped with 1 mL of water, and the mixture was centrifuged. It was then washed with DMF, water, and acetone three times each to get rid of the unattached carboxyfluorescein and finally was centrifuged. The nanoparticles were finally dried under vacuum.

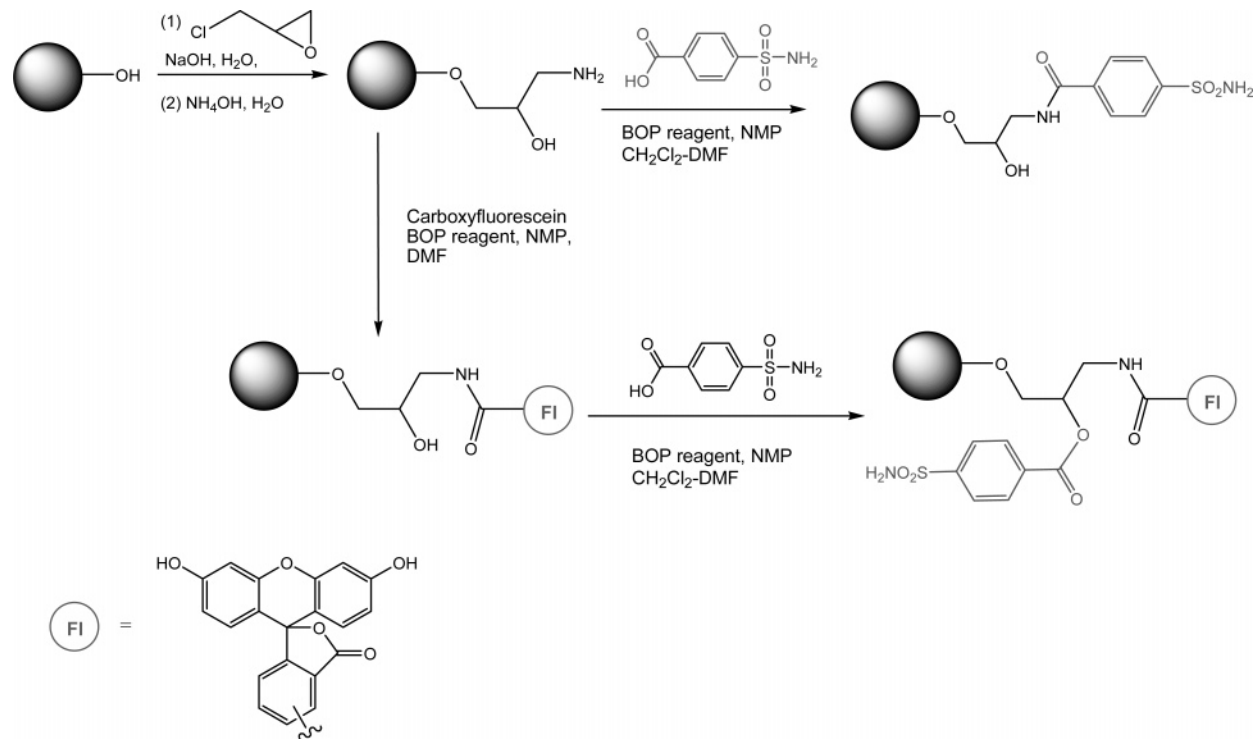
The carboxyfluorescein-functionalized nanoparticles were taken through the same procedure to attach additional CBS. This resulted in nanoparticles functionalized with carboxybenzenesulfonamide, as well as particles with both the CBS and carboxyfluorescein as shown in Scheme 1.

X-ray Photoelectron Spectroscopy (XPS). The surface functionalization chemistry of the nanoceria was examined using a 5400 PHI ESCA (XPS) spectrophotometer. The base pressure during the XPS analysis was approximately 10⁻⁹ Torr, and Mg K α X-radiation (1253.6 eV) at a power of 200 W was used. The instrument was calibrated using a standard gold sample with the binding energy at 84.0 \pm 0.1 eV for Au (4f_{7/2}). All the samples were placed on a carbon tape. Any charging shift produced during the scanning was subtracted by using a binding energy scale with the baseline set at 284.6 eV for the C (1s).²⁷ The XPS spectra were deconvoluted using PeakFit (version 4) software. The surface concentration of various conjugates was evaluated from the integrated areas of the peaks corresponding to the respective conjugates.

Confocal Fluorescence Microscopy (CFM). An Olympus Fluoroview IX 81 confocal fluorescence microscope was used. The imaging was performed by preparing slides with nanoceria samples functionalized by carboxyfluorescein. The concentration of nanoceria was optimized to 1 mg/mL of water for imaging. The emission and excitation wavelengths for carboxyfluorescein were determined to be 520 and 480 nm, respectively.

Ultraviolet–Visible Spectrophotometry (UV–vis). Cary 1E UV–vis spectrophotometer (UV–vis) from Varian Inc. was used to determine the inhibition potential of the nanoceria

SCHEME 1: The Synthesis of the Functionalized Nanoceria



functionalized with CBS. The enzyme activity was measured in 25 mM HEPES buffer, pH 7.0 at 25 °C, containing 10% acetonitrile. The concentration of hCAII (obtained from Sigma-Aldrich Company) was kept constant at 1 μ M for all the experiments. The concentration of the substrate, 4-nitrophenyl acetate (in acetonitrile), was 1 mM for experiments carried out with varying concentrations of functionalized nanoceria and varied between 1 and 5 mM for the kinetic parameter determination studies with constant concentration of the functionalized nanoceria at 0.16667 mg/mL. The initial rates of 4-nitrophenyl acetate hydrolysis by hCAII were monitored spectrophotometrically, at 400 nm, using the Cary WinUV Kinetics application. The molar absorption coefficient, ϵ of 18 400 $M^{-1} \text{ cm}^{-1}$, was used to determine the concentration of 4-nitrophenolate formed by hydrolysis, as reported in the literature.²⁸

The substrate concentration dependent kinetic data in the absence and presence of functionalized-nanoceria inhibitors was presented in the form of double reciprocal plots and was analyzed according to the Michaelis–Menten equation to obtain the K_m and V_{max} values. The inhibitor binding constant, K_i , for the functionalized-nanoceria inhibitors was determined according to the following relationship:²⁹

$$K_i = \frac{K_m[I]}{K_m' - K_m} \quad (1)$$

where, [I] is inhibitor (functionalized-nanoceria) concentration; K_m and K_m' are Michaelis constants in the absence and presence of the inhibitor, respectively.

Results

The expected functionalization of nanoceria was confirmed by XPS. The attachments of the epichlorohydrin linker, the inhibitor, and the fluorophore were established by examining the high-resolution C (1s) and O (1s) XPS spectra. The attachment of the fluorophore-functionalized nanoparticles was further confirmed by imaging using a confocal fluorescence microscope.

Functionalization Chemistry Using X-ray Photoelectron Spectroscopy (XPS). The carboxybenzenesulfonamide and carboxyfluorescein were conjugated by first attaching epichlorohydrin to the surface of nanoceria particles. This is a standard S_N2 reaction where the oxygen atom of the nanoceria essentially replaces the chlorine atom of the epichlorohydrin.³⁰ This results in an oxygen atom that bonds the cerium with the carbon of the epichlorohydrin as seen in the first reaction of Scheme 1.

In case of nanocrystalline cerium oxide, the O (1s) spectra contain two peaks corresponding to the mixed valence state of Ce (Ce^{3+} and Ce^{4+}) present in its crystal lattice. The peak at 530.5 eV corresponds to Ce^{4+} while the higher binding energy peak at about 532.20 eV corresponds to Ce^{3+} .³¹ The two additional peaks present in the spectra given in Figure 3a demonstrate that the expected functionalization occurred. These peaks include the O (1s) line of the epichlorohydrin's epoxy group at 533.30 eV and the O–C bond that connects the main part of the epichlorohydrin molecule to the cerium oxide at 534.10 eV.³² The high-resolution O (1s) XPS spectra thus indicate the successful attachment of the epichlorohydrin molecule to cerium oxide nanoparticles. The loading of epichlorohydrin on the ceria nanoparticles, calculated from the integrated areas of O peaks corresponding to epichlorohydrin to those for Ce^{3+} and Ce^{4+} , was evaluated to be 3.18 mmol/gm of CeO_2 .

Next, ammonia was used to open up the epoxide ring (S_N2 reaction) on the epichlorohydrin molecule to form amine ($-NH_2$) and hydroxyl ($-OH$) groups available for further reactions (Scheme 1). The indication that this reaction occurred lies in the diminishment of the peak at 533.30 from Figure 3a. The new peak at 533.00 eV in Figure 3b corresponds to the newly formed $-OH$ groups.³² However, Figure 3b also confirms that the O–C bond that links the epichlorohydrin molecule bond to the nanoceria remained with the peak at 534.00 eV. Thus, the epichlorohydrin was still attached to the nanoceria and the epoxide ring opened as expected. The integrated area analysis of the peaks confirmed almost 100% ring opening for the

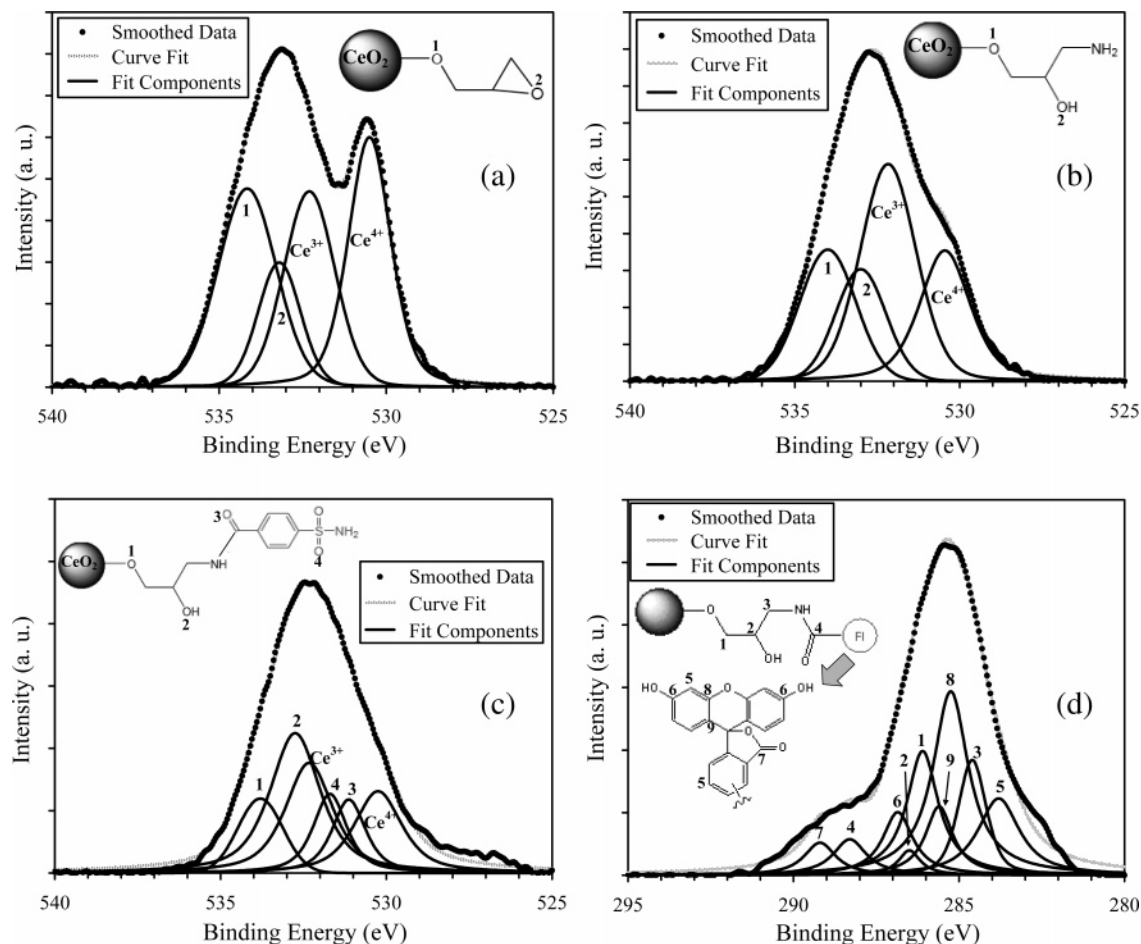


Figure 3. High-resolution XPS spectra for the functionalized nanoceria particles at various conjugation steps. (a) O 1s scan for epichlorohydrin-functionalized nanoceria. (b) O 1s scan for the opened epoxide ring of epichlorohydrin. (c) O 1s scan for carboxybenzenesulfonamide-functionalized nanoceria. (d) C 1s scan for carboxyfluorescein-functionalized nanoceria. (The peak positions are listed in Table S1 of the Supporting Information.)

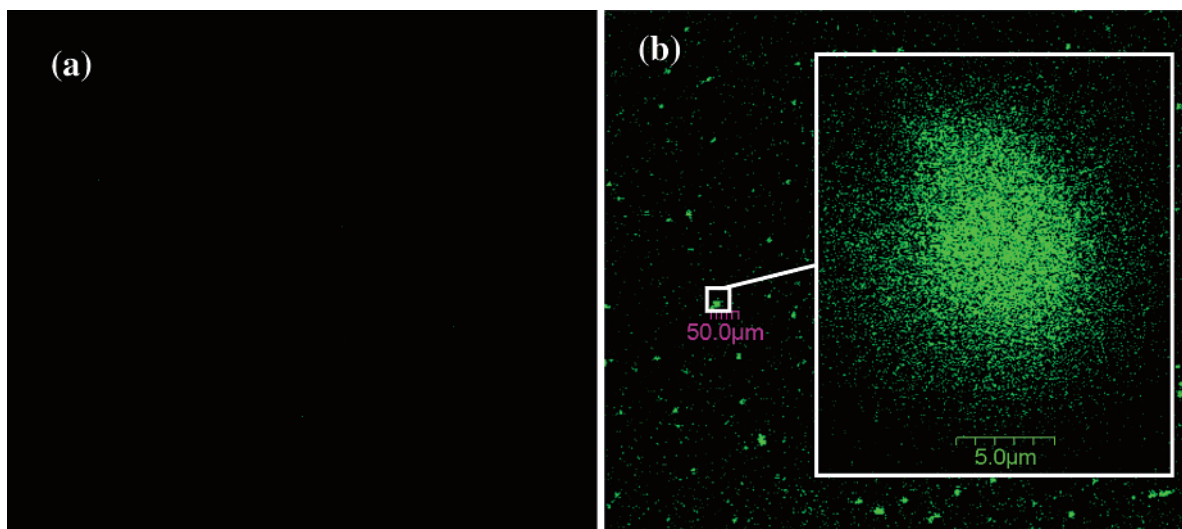


Figure 4. Confocal fluorescence microscopy images of (a) bare nanoceria and (b) nanoceria with fluorophores.

epoxide group of the epichlorohydrin conjugated to the cerium oxide nanoparticles.

The nanoceria now possessed two functional groups that could be functionalized by the carboxybenzenesulfonamide and carboxyfluorescein molecules. Both of them have carboxyl groups that can react to the available amine and hydroxyl groups from the opened ring of the surface-functionalized nanoceria (Figure 2). The coupling reactions included standard peptide coupling reagents, *N*-methyl morpholine (NMP) and benzotriazol-1-yl-

oxy-tris-(dimethylamino) phosphonium hexafluorophosphate (BOP). The reactions were conducted in dimethylformamide (DMF), a polar aprotic solvent that facilitates the coupling.³³

Next, the attachment of the inhibitor, CBS, to the amine group was confirmed by the O 1s XPS spectrum in Figure 3c. The locations of all of the peaks essentially remained the same from the previous spectrum in Figure 3b except for two additional peaks. These peaks at 531.13 and 531.70 eV correspond to the double-bonded oxygen atoms of the C=O and S=O bonds,

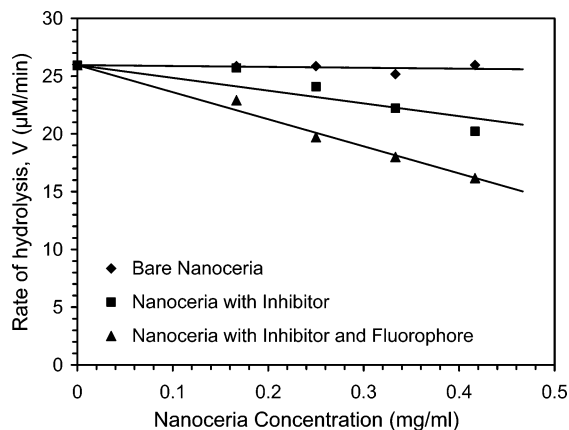


Figure 5. The rate of the hydrolysis of 4-nitrophenyl acetate by hCAII (determined using absorbance change at 400 nm) as a function of the nanoceria concentration.

respectively, that are part of the CBS.³² The XPS analysis thus indicated that the inhibitor bonded to the nanoceria particles. The loading yield determined from the deconvoluted peak areas was evaluated to be 3.14 mmol/gm of CeO₂ (98.8%).

Last, instead of the O 1s spectrum, the carbon (C 1s) spectrum was used to confirm the attachment of carboxyfluorescein, because this large molecule shielded many of the oxygen peaks seen in the previous oxygen spectra. Figure 3d shows the various peaks present in the XPS spectra corresponding to the different C positions in the structure of the carboxyfluorescein-functionalized ceria nanoparticles. It confirms that the fluorophore was also attached successfully to the ceria nanoparticles via epichlorohydrin linkage. The XPS peak analysis gave the surface concentration of the fluorophore to be 6.0 mmol/gm of CeO₂. The results of the high-resolution XPS spectra for all of the reactions are summarized in Table S1 of the Supporting Information.

Confocal Fluorescence Microscopy. Further evidence that the fluorescent molecules bonded was presented in the confocal fluorescence microscopy images. As seen in Figure 4, the carboxyfluorescein-functionalized nanoparticles were clearly visible under a confocal fluorescence microscope ($\lambda_{\text{ex}} = 480$ nm; $\lambda_{\text{em}} = 520$ nm) as green dots while the bare nanoceria resulted in images showing a black background. An individual green dot represents a small agglomerate of the ceria nanoparticles (particle size: 10–20 nm) successfully functionalized with carboxyfluorescein. This further demonstrates that the fluorophores were attached to the nanoceria. The procedure for attaching these fluorescent molecules can be used in future studies to track the nanoceria as they are inserted into living cells. Future studies will involve inserting these particles in vivo and tracking their movement as they approach the expected locations of enzymes.

Inhibition Studies. The final facet of the study involved determining whether the functionalized nanoceria inhibited the recombinant hCAII enzyme. This was accomplished by observing the effect of nanoparticles on the rate of hCAII-catalyzed hydrolysis of the substrate 4-nitrophenyl acetate. Essentially, the nanoparticles were mixed with a solution of the 4-nitrophenyl

acetate and enzyme. The UV–vis spectrophotometer then measured the absorbance values at 400 nm as 4-nitrophenylacetate was hydrolyzed to form 4-nitrophenolate.²⁸ The change in the absorbance values at different concentrations of nanoceria indicated the inhibiting effect of the conjugated nanoparticles.⁸

The declining slopes in Figure 5 reveal that, when the inhibitor-functionalized nanoceria bound to the active site of hCAII, the rate of formation of 4-nitrophenolate from 4-nitrophenyl acetate decreased.⁸ A decrease in the rate of its formation produced a solution that became tinted at a slower rate, which was represented by the decrease in the absorbance values as a function of time (see Figure 5). hCAII's activity declined with increased concentration of nanoceria, as indicated by the decreasing rate for the hydrolysis of 4-nitrophenyl acetate to 4-nitrophenolate. Bare nanoceria did not affect the rate of hydrolysis of 4-nitrophenyl acetate. When the inhibitor was paired with the fluorophore, the inhibition was better than with nanoceria functionalized only with CBS. The kinetic parameters (K_m , V_{max} , and K_i) for the functionalized-nanoceria samples, determined using the double-reciprocal plots, are summarized in Table 1.

Discussion

One of the emerging goals of nanotechnology is to functionalize inert and biocompatible materials to impart precise biological functions. Several hybrid organic/inorganic nanoparticles have been described for diagnostic or therapeutic use,^{34,35} including quantum dots,^{36,37} polymers,³⁸ and magnetofluorescent nanoparticles.³⁹ Although many coupling systems have been reported for polymeric nanoparticle conjugation with varying degrees of success,^{40,41} the coupling and functionalization of inorganic nanoparticles with biomolecules has only been carried out with a limited number of chemical methods. Niemeyer⁴² has written an elaborate review on usage of various coupling agents such as citrate, streptavidin, and various other complex linker molecules with amide and carboxylic acid end groups for coupling of inorganic nanoparticles (Au, Ag, ZnS, CdS, SnO₂, TiO₂, etc.) with biomolecules (proteins, DNA, etc.).

In this study, we have shown the simultaneous conjugation of the hCAII inhibitor, CBS, and the fluorophore, carboxyfluorescein, to cerium oxide nanoparticles via epichlorohydrin as a linker molecule. Epichlorohydrin is a highly reactive compound used in manufacture of epoxy and phenoxy resins. It is also used as a solvent and in the synthesis of glycerol. Anirudhan et al.⁴³ have developed a new adsorbent system for phosphate removal from wastewaters using epichlorohydrin to modify lignocellulosic residue. Also, it has been used in synthesis of lipopolyhydroxylalkylamines for gene delivery.⁴⁴ Weissleder et al.⁴⁵ cross-linked the monocrySTALLINE magnetic nanoparticles, consisting of 3 nm core of (Fe₂O₃)_n(Fe₃O₄)_m covered with a layer of dextran, with epichlorohydrin and aminated them by reaction with ammonia to provide primary amine groups for the parallel synthesis of a library comprising 146 nanoparticles decorated with different synthetic small molecules. Similarly, in the present study, epichlorohydrin was attached to the ceria nanoparticles via a condensation reaction between the organochloride group from epichlorohydrin and the surface hydroxyl

TABLE 1: Kinetic Parameters of the hCAII-Catalyzed Reaction in the Absence and Presence of Functionalized-Nanoceria Inhibitors

inhibitor	K_m (mM)	V_{max} (mM/min)	K_i (mg/mL)
no inhibitor	115.23 ± 1.36	3.02 ± 0.15	
nanoceria with inhibitor (CBS)	125.40 ± 0.98	3.24 ± 0.08	1.89 ± 0.16
nanoceria with inhibitor (CBS) and fluorophore (carboxyfluorescein)	135.24 ± 1.10	3.12 ± 0.10	0.96 ± 0.09

groups of the nanoceria particles and then was aminated to provide primary amine group for conjugation of enzyme inhibitor as well as the fluorophore to the nanoceria particles.

The epichlorohydrin may have provided a spacer that allowed the inhibitor to reach the active site of the carbonic anhydrase and to reduce any steric hindrance of the enzyme's interaction with the inhibitors on the surface of the nanoparticles. Furthermore, the inhibition was nearly directly proportional with increased concentration of the functionalized-nanoceria inhibitors (Figure 5). The analysis of the kinetic data conformed to the competitive type of inhibition model. Higher K_m values in the presence of functionalized-nanoceria inhibitors than in its absence eliminate the possibility of "noncompetitive inhibition". In conclusion, these preliminary results demonstrate that an inhibition of the hCAII enzyme can be achieved using nanoceria particles, surface-functionalized with CBS.

The aim of the present study was to show that a successful conjugation of the ceria nanoparticles can be carried out using epichlorohydrin as a linker molecule and such conjugated nanoparticles can be used for hCAII inhibition along with fluorescence-imaging capabilities. The inhibition results can be further enhanced using multiprong surface-binding groups. Our earlier studies in this regard have shown a strategy to improve inhibition of hCAII by attaching a surface-histidine recognition group to the inhibitor. Future studies will include the usage of the same conjugation process for multiprong inhibitors of hCAII for improved results.

Conclusion

Nanoceria were successfully functionalized and tested as inhibitors for hCAII. High-resolution XPS C 1s and O 1s spectra were effectively utilized to follow the necessary steps in the reaction process. The fluorescence microscope images and quantitative observations further confirmed that the carboxy-fluorescein molecules bonded to the nanoceria particles. These results are very promising, and more studies will likely evolve into an inhibition of hCAII in living cells and an effective treatment of glaucoma and other diseases. Furthermore, inhibitors for other pathogenic enzymes can be immobilized on the nanoceria and then applied to the enzymes. The potential applications for functionalized cerium oxide nanoparticles seem limitless as a potential nontoxic drug delivery tool.

Acknowledgment. We thank the National Science Foundation EEC 0453436; BES 0541516 for providing the funding to make this research possible. Thank you to Dr. D. K. Srivastava for allowing the use of his laboratory for inhibition studies. Last, thanks to Rajesh Subramaniam and Joel Koorean for their help with the fluorescence microscope and UV-vis, respectively. S.P. and S.R. contributed equally to this work.

Supporting Information Available: The peak positions for the various deconvoluted XPS spectra of the functionalized nanoceria particles (Figure 3) have been summarized in Table S1. This material is available free of charge via the Internet at <http://pubs.acs.org>.

References and Notes

- Mann, T.; Keilin, D. *Nature* **1940**, *146*, 164–165.
- Beasley, Y. M.; Overell, B. G.; Petrow, V.; Stephenson, O. *J. Pharm. Pharmacol.* **1958**, *10*, 696–705.
- Mincione, F.; Starnotti, M.; Menabuoni, L.; Scozzafava, A.; Casini, A.; Supuran, C. T. *Bioorg. Med. Chem. Lett.* **2001**, *11*, 1787–1791.
- Boriack, P. A.; Christianson, D. W.; Kingery-Wood, J.; Whitesides, G. M. *J. Med. Chem.* **1995**, *38*, 2286–2291.
- Poulsen, S. A.; Bornaghi, L. F.; Healy, P. C. *Bioorganic & Medicinal Chemistry Letters* **2005**, *15*, 5429–5433.
- Gryzbowski, B. A.; Ishchenko, A. V.; Kim, C. Y.; Topalov, G.; Chapman, R.; Christianson, D. W.; Whitesides, G. M.; Shakhnovich, E. I. *Proc. Natl. Acad. Sci. U.S.A.* **2002**, *99*, 1270–1273.
- Sigal, G. B.; Whitesides, G. M. *Bioorg. Med. Chem. Lett.* **1996**, *6*, 559–564.
- Roy, B. C.; Banerjee, A. L.; Swanson, M.; Jia, X. G.; Haldar, M. K.; Mallik, S.; Srivastava, D. K. *J. Am. Chem. Soc.* **2004**, *126*, 13206–13207.
- Ilies, M.; Supuran, C. T.; Scozzafava, A.; Casini, A.; Mincione, F.; Menabuoni, L.; Caproiu, M. T.; Maganu, M.; Banciu, M. D. *Bioorg. Med. Chem.* **2000**, *8*, 2145–2155.
- Fridborg, K.; Kannan, K. K.; Liljas, A.; Lundin, J.; Strandberg, B.; Strandberg, B.; Tilander, T. L. B.; Wiren, G. *J. Mol. Biol.* **1967**, *25*, 505–514.
- Day, Y. S. N.; Baird, C. L.; Rich, R. L.; Myszka, D. G. *Protein Sci.* **2002**, *11*, 1017–1025.
- Zimmer, A.; Kreuter, J. *Adv. Drug Delivery Rev.* **1995**, *16*, 61–73.
- Lee, V. H. L.; Robinson, J. R. *J. Pharm. Sci.* **1979**, *68*, 673–684.
- Patton, T. F.; Robinson, J. R. *J. Pharm. Sci.* **1976**, *65*, 1295–1301.
- Zimmer, A.; Mutschler, E.; Lambrecht, G.; Mayer, D.; Kreuter, J. *Pharm. Res.* **1994**, *11*, 1435–1442.
- Harmia, T.; Speiser, P.; Kreuter, J. *Int. J. Pharm.* **1986**, *33*, 45–54.
- Vidmar, V.; Pepeljnjak, S.; Jalsenjak, I. *J. Microencapsulation* **1985**, *2*, 289–92.
- Zimmer, A. K.; Zerbe, H.; Kreuter, J. *J. Controlled Release* **1994**, *32*, 57–70.
- Kim, C. K.; Oh, Y. K. *Int. J. Pharm.* **1988**, *47*, 163–169.
- Rzagalinski, B. A.; Bailey, D.; Chow, L.; Kuiry, S. C.; Patil, S.; Merchant, S.; Seal, S. *FASEB J.* **2003**, *17*, A606–A606.
- Tarnuzzer, R. W.; Colon, J.; Patil, S.; Seal, S. *Nano Lett.* **2005**, *5*, 2573–2577.
- Chen, J.; Patil, S.; Seal, S.; McGinnis, J. F. *Nat. Nanotechnol.* **2006**, *1*, 142–150.
- Limbach, L. K.; Li, Y. C.; Grass, R. N.; Brunner, T. J.; Hintermann, M. A.; Muller, M.; Gunther, D.; Stark, W. J. *Environ. Sci. Technol.* **2005**, *39*, 9370–9376.
- Banerjee, A. L.; Tobwala, S.; Haldar, M. K.; Swanson, M.; Roy, B. C.; Mallik, S.; Srivastava, D. K. *Chem. Commun.* **2005**, 2549–2551.
- Pittet, M. J.; Swirski, F. K.; Reynolds, F.; Josephson, L.; Weissleder, R. *Nat. Protoc.* **2006**, *1*, 73–79.
- Polat, M. F.; Nalbantoglu, B. *Turk. J. Med. Sci.* **2002**, *32*, 299–302.
- Barr, T. L.; Seal, S. *J. Vac. Sci. Technol., A: Vac. Surf. Films* **1995**, *13*, 1239–1246.
- Scozzafava, A.; Supuran, C. T. *Bioorg. Med. Chem.* **2003**, *11*, 2241–2246.
- Roy, B. C.; Hegge, R.; Rosendahl, T.; Jia, X.; Lareau, R.; Mallik, S.; Srivastava, D. K. *Chem. Commun.* **2003**, 2328–2329.
- Smith, A. B.; Pitram, S. M.; Boldi, A. M.; Gaunt, M. J.; Sfougataki, C.; Moser, W. H. *J. Am. Chem. Soc.* **2003**, *125*, 14435–14445.
- Henderson, M. A.; Perkins, C. L.; Engelhard, M. H.; Thevuthasan, S.; Peden, C. H. F. *Surf. Sci.* **2003**, *526*, 1–18.
- Beamson, G.; Briggs, D. *High Resolution XPS of Organic Polymers*; John Wiley & Sons: New York, 1992.
- Brown, W. H. *Introduction to Organic Chemistry*; Saunders College Publishing: Philadelphia, PA, 2000.
- Whitesides, G. M. *Nat. Biotechnol.* **2003**, *21*, 1161–1165.
- Nam, J. M.; Thaxton, C. S.; Mirkin, C. A. *Science* **2003**, *301*, 1884–1886.
- Zorov, D. B.; Kobrin, E.; Juhaszova, M.; Sollott, S. J. *Circ. Res.* **2004**, *95*, 239–252.
- Santra, S.; Yang, H. S.; Holloway, P. H.; Stanley, J. T.; Mericle, R. A. *J. Am. Chem. Soc.* **2005**, *127*, 1656–1657.
- Modo, M.; Mellodew, K.; Cash, D.; Fraser, S. E.; Meade, T. J.; Price, J.; Williams, S. C. R. *Neuroimage* **2004**, *21*, 311–317.
- Josephson, L.; Kircher, M. F.; Mahmood, U.; Tang, Y.; Weissleder, R. *Bioconjugate Chem.* **2002**, *13*, 554–560.
- Najera, C. *Synlett* **2002**, 1388–1403.
- Valeur, E.; Bradley, M. *Chem. Commun.* **2005**, 1164–1166.
- Niemeyer, C. M. *Angew. Chem., Int. Ed.* **2001**, *40*, 4128–4158.
- Anirudhan, T. S.; Noeline, B. F.; Mancihar, D. M. *Environ. Sci. Technol.* **2006**, *40*, 2740–2745.
- Li, Q.; Zhang, G. S.; Marhefka, J.; Kameneva, M. V.; Liu, D. X. *Bioorg. Med. Chem. Lett.* **2006**, *16*, 2428–2432.
- Weissleder, R.; Kelly, K.; Sun, E. Y.; Shtatland, T.; Josephson, L. *Nat. Biotechnol.* **2005**, *23*, 1418–1423.